Comparison of coherence and phase synchronization of the human sleep electroencephalogram

Kristína Mezeiová [a,b], Milan Paluš [b,*],

[a] *Institute of Measurement Science, Slovak Academy of Sciences, Dúbravská cesta 9, 841 04 Bratislava, Slovak Republic*
[b] *Institute of Computer Science, Academy of Sciences of the Czech Republic, Pod vodárenskou věží 2, 182 07 Prague 8, Czech Republic*

Abstract

Objective: Potential differences between coherence and phase synchronization analyses of human sleep electroencephalogram (EEG) are assessed and occurrences of phase vs. complete synchronization between EEG signals from different locations during different sleep stages are investigated.

Methods: Linear spectral coherence, mean phase coherence (MPC) z-score and Pearson's correlation coefficient of analytic amplitudes were evaluated for different spectral bands of whole-night EEG recordings from 25 healthy subjects.

Results: Coherence and MPC z-score demonstrated practically the same statistical differences between vigilance stages, confirming the findings of previous coherence-based studies. MPC z-score and amplitude correlations were most correlated (>0.5) between homologous interhemispheric positions and least correlated between nonhomologous interhemispheric positions and between fronto-occipital positions.

Conclusions: Coherence and phase synchronization provided essentially the same information. Complete synchronization was manifested by highly coherent phases and correlated amplitudes, as well as by correlated changes of phase synchronization, coherence and amplitude correlations between vigilance states. In cases of weaker coupling, phase synchronization and coherence change in agreement, while behaviour of amplitude correlations differs.

Significance: Phase synchronization analysis is not superior to coherence analysis, although the coupling between EEG signals is dominated by phase synchronization which turns into complete synchronization in the most strongly coupled EEG signals.

Key words: Phase synchronization; Complete synchronization; Mean phase coherence; Permutation surrogate data; Coherence; Human sleep EEG

Highlights:

- Coherence and phase synchronization analyses yield practically the same statistical differences between stages of human sleep EEG.
- Coupling between EEG signals is dominated by phase synchronization which turns into complete synchronization in the most strongly coupled EEG signals.
- In gamma band the type of synchronization depends on sleep state, while in other spectral bands it is determined by topographic positions of considered electrodes.

* Corresponding author.
Email address: mp@cs.cas.cz (Milan Paluš).

Clinical Neurophysiology, 123 (9) (2012) 1821-1830 *doi:10.1016/j.clinph.2012.01.016*

1. Introduction

Analysis of synchronization between EEG signals attempts to detect and describe coordination between different areas of the cortex (Gray et al., 1989; Roelfsema et al., 1997). During sleep synchronous oscillatory activity appears at several frequencies (Steriade et al., 1991, 1993a,b). Investigation of these phenomena has been done mostly by the means of coherence (Dumermuth and Lehmann, 1981; Dumermuth et al., 1983; Achermann and Borbély, 1998a; Duckrow and Zaveri, 2005) which is a measure of linear covariance between the cross-spectra of two signals.

The concept of phase synchronization (Rosenblum et al., 1996) draws from the study of chaotic and/or noisy, weakly coupled oscillators and generalizes the phenomenon of phase locking. The difference of instantaneous phases of two synchronized oscillators remains constant during their phase-locked state. In the case of real, chaotic and/or noisy systems the phase difference is subject to numerous perturbations and the phase-locking condition can be relaxed as:

$$|n\Phi_x - m\Phi_y| < const \tag{1}$$

where Φ_x, Φ_y are instantaneous phases of signals x, y and n, m are generally natural numbers, in the case of EEG $n = m = 1$ is usually considered. Phase synchronization means an entrainment of phases, while the amplitudes of phase-synchronized systems can be uncorrelated (Rosenblum et al., 1996).

Complete synchronization is a state when the states of both oscillatory systems become topologically identical - phases and amplitudes of the two oscillators are strongly correlated. The different types of synchronization appear in dependence on the strength of coupling between the two systems: the oscillatory processes are uncorrelated when there is no coupling between them, phase synchronization appears between weakly coupled oscillators, and the complete synchronization comes out when the coupling strength increases above some threshold (Osipov et al., 2003).

Phase synchronization analysis was introduced into the area of EEG signal processing by Lachaux et al. (1999) and Mormann et al. (2000), recent applications include investigation of cognitive processes – visual perception, mental rotation (Bhattacharya et al., 2001), or pathological states such as epileptic seizures (Mormann et al., 2000), schizophrenia (Bob et al., 2008; Spencer et al., 2003), attention deficit (hyperactivity) disorder (Tcheslavski and Beex, 2006) or migraine (Angelini et al., 2004).

According to Lachaux et al. (1999) the phase synchronization analysis is preferable to coherence analysis in estimation of synchronization phenomena as it is a function of pure phase differences, independent of amplitudes of spectra. Also, phase information is generally considered to be "purer" or more informative than the amplitude of EEG, which is more influenced by the impedance of the skull or various artifacts such as eyes or face muscles movements (Galka, 2000).

The role of phase synchronization in neuroscience, however, goes far beyond an analysis technique. Looking for explanation of large-scale integration that counterbalances the distributed anatomical and functional organization of brain activity, phase synchronization is considered as a plausible candidate for a mechanism suitable for establishing dynamical links between distant brain areas over multiple frequency bands (Varela et al., 2001). The possible long-range character of phase synchronization indicates that phase synchrony, particularly in the gamma band, can be the fundamental process that subserves large-scale cognitive integration (Rodriguez et al., 1999) and cortical computation (Fries, 2009). Phase synchronization analysis and coherence analysis are both sensitive to detect phase synchrony over multiple frequency bands, however, their are not specific in detecting the correct class of underlying physical mechanism (Winterhalder et al., 2006).

The main objectives of this study are (i) to investigate, in the context of the human sleep EEG, whether phase synchronization analysis can give more information than the conventionally used coherence analysis and (ii) whether phase synchronization or complete synchronization of EEG signals occurs in different vigilance/sleep stages.

2. Methods

2.1. *Data*

Whole-night polysomnographic recordings with sleep stage scorings according to Rechtschaffen - Kales criteria (Rechtschaffen and Kales, 1968) were kindly provided by Prof. G. Dorffner, from The Siesta Group Schlafanalyse GmbH. The data was recorded within the project SIESTA funded by the European Commission. Written informed consent was obtained from each subject. Recordings consisted of electroencephalogram (EEG), electrooculogram (EOG), electromyogram (EMG), electrocardiogram (ECG) and respiratory signals. The signals were visually checked by experts and sleep stages were scored using 30s long epochs. Details about measurement conditions and parameters of the signals can be found in (Anderer et al., 2005). No further preprocessing has been done in this study.

In the present study EEG recordings from 25 healthy adult subjects (12 males, mean age 50 years, range from 23 to 82 years) were analyzed; subjects spent two nights in the sleep laboratory. Signals were sampled at 256 Hz, high-pass filtered with the cut-off frequency of 0.1 Hz, low-pass filtered with cut-off frequency of 75 Hz, and notch filtered at 50 Hz. Electrodes with the reference on the contralateral mastoid were placed on the following positions according to the International 10-20 system: Fp1/M2, C3/M2, O1/M2, Fp2/M1, C4/M1, O2/M1, and M1/M2 for re-referencing. In our notation the slash symbol "/" is used to distinguish the symbols of the two electrode locations from which the resulting signal was derived. For the unipolar (common reference) signals the notation X/Y simply means the electrode position of interest (X) and its reference electrode (Y). For bipolar derivations the meaning of the X/Y notations is defined by the formulae given below. The bipolar derivations were calculated in order to remove the influence of the referential electrode and most of the volume conduction (Fein et al., 1988; Nunez et al., 1997; Rappelsberger, 2000) on the value of each of the dependence measures. Four intrahemispheric signals along the antero-posterior axis Fp1/C3, Fp2/C4, C3/O1, C4/O2 were obtained as differences of signals with the same reference electrode: $X_i/Y_i = X_i/M_j - Y_i/M_j$, where X, Y is a frontal, central or occipital electrode, i and j denote the position on the right or left hemisphere. Three derivations along the dextro-sinistral axis – Fp1/Fp2, C3/C4, O1/O2 – were attained by the use of M1/M2 signal as: $X_i/X_j = X_i/M_j - X_j/M_i + M1/M2$.

2.2. *Phase synchronization*

The first step in phase synchronization analysis is the extraction of instantaneous phases from the systems under study. In the literature there are two methods of phase extraction commonly used - the analytic signal concept of Gabor (1946) with Hilbert transform and wavelet transform. Le Van Quyen et al. (2001); Paluš et al. (2005) showed that applications of the both methods lead to equivalent results. As Hilbert transform is a unit gain filter at each frequency, broad-band signals like EEG should be pre-filtered to the frequency band of interest. On the other hand, wavelet transform can be considered as band-pass filter and the pre-filtering would be redundant. In this work the phase of the signals was extracted by the convolution with complex Morlet wavelet (Torrence and Compo, 1998):

$$W(t,f) = \int_{-\infty}^{\infty} \psi(t')x(t-t')dt' = A(t)e^{i\phi(t)} \tag{2}$$

$$\psi(t) = \frac{1}{\sqrt{2\pi\sigma_t^2}} \exp(-\frac{t^2}{2\sigma_t^2}) \exp(2\pi i f_0), \tag{3}$$

where $\psi(t)$ is the complex Morlet wavelet, x is the signal (EEG), $A(t)$ and $\phi(t)$ are complex amplitude and phase of x, σ_t is the bandwidth parameter, and f_0 is the central frequency of the wavelet. σ_t determines the rate of decay of Gauss function, its reciprocal value $\sigma_f = 1/\pi\sigma_t$ determines the spectral bandwidth.

In this study, following central frequencies f_0 and spectral bandwidth σ_f (the latter given in the parentheses), which cover main frequency bands used in sleep research, were used
$f_0(\sigma_f)$: δ: 2(1) Hz, θ: 6(2) Hz, α: 10 (2) Hz, σ: 14(3) Hz, β: 22(7) Hz, and γ: 35(7) Hz.

Working with time series, the phase locking condition (1) is evaluated in a statistical sense. One of the measures that quantify the distribution of phase differences is the mean phase coherence (MPC) (Mormann et al., 2000):

$$R = \sqrt{| < \exp(i\phi_{xy}(t)) > |} \tag{4}$$

where $\phi_{xy}(t)$ is the difference between the instantaneous phases of signals x and y and $<>$ means time averaging. If the two signals are phase synchronized most of the time, the relative phase will occupy a small portion of the unit circle and the mean phase coherence is close to $R = 1$. On the contrary a uniform distribution of phases (which would be expected, on average, for asynchronous time series) results in $R = 0$. Such clear distinction, however, is only theoretical. Analysing phases from real, noisy data, any value between 0 and 1 can be obtained. Moreover, the MPC values can be biased according to properties of the analysed signals, such as their frequency distribution (Xu et al., 2006).

Therefore further statistical evaluation of the MPC values is necessary. Reliability of the level of phase synchrony is evaluated by using the surrogate data approach (Theiler et al., 1992; Paluš, 1995) which is a formal statistical test with the null hypothesis that the value of original data is not significantly different from the specific class of signals. Good surrogate data are constructed so that they mimic all properties of the signals, but destroy only the one property suspected to be the source of outstanding values of measure computed. Assuming normal distribution of computed measure of surrogates, the statistical test can be evaluated with the z-score statistic. Z-score statistic counts how different is the value of original data from the mean value of all surrogates μ in the units of standard deviation (SD):

$$z = \frac{R_{EEG} - \mu(R_{Surr})}{SD(R_{Surr})} \tag{5}$$

In this study permutation surrogate data (Vejmelka and Paluš, 2008) were used. They are constructed, for each frequency band, from the phase time series by random permutation of the time blocks given by single cycles of variable period. Permutation surrogate data preserve phase and period distribution, but destroy the temporal dynamics between the cycles. Thus, using the z-scores, possible bias in MPC is corrected and the null hypothesis of independence of the phases is tested. From each sleep epoch an ensemble of 100 permutation surrogate data was constructed and the z-score statistic was computed.

2.3. *Coherence*

30s long segments of signals were divided into 2s long nonoverlapping parts. A Hamming window was applied to each of them, and average auto- and cross- spectra were computed. Magnitude squared coherence for the k_{th} frequency band was taken as the value of the cross-spectrum normalized by the values of the auto-spectra:

$$\kappa^2_{xy}(\bar{k}) = \frac{|\sum\limits_k P_{xy}(k)|^2}{\sum\limits_k P_{xx}(k) \sum\limits_k P_{yy}(k)} \tag{6}$$

where the summation went through all the frequencies belonging to the given frequency band $\bar{k}$ (Andrew and Pfurtscheller, 1996). Coherence was computed for the following frequency bands δ: 1–3 Hz, θ: 4–8 Hz, α: 8–10 Hz, σ: 11–17 Hz, β: 15–29 Hz, and γ: 28–42 Hz.

2.4. *Correlation coefficient between amplitudes*

In order to investigate whether also the instantaneous amplitudes are synchronized and complete synchronization occurs, Pearson's correlation coefficient of the instantaneous amplitudes acquired with the convolution with the complex Morlet wavelet (see Equation 2) was computed:

$$\rho_A(x,y) = \frac{E\left[\left(A_x(t) - \mu(A_x(t))\right)\left(A_y(t) - \mu(A_y(t))\right)\right]}{SD\left(A_x(t)\right) SD\left(A_y(t)\right)}$$

where E is expected value, $A_X(t)$, $A_Y(t)$ are instantaneous amplitudes of signals X and Y, μ is mean and SD is the standard deviation.

2.5. *Statistical analysis*

Statistical analysis was performed by means of three-way repeated measures ANOVA with factors stage, position, and band. The factor stage included wakefulness (7008 epochs), nonREM sleep (consisted of nonREM sleep stages 2, 3 and 4; 25 090 epochs) and REM sleep (6653 epochs). The factor position included values computed between following signals: Fp1/C3–Fp2/C4, C3/O1–C4/O2 (interhemispheric homologous derivations), Fp1/C3–C4/O2, C3/O1–Fp2/C4 (interhemispheric nonhomologous derivations) and between Fp1/Fp2–C3/C4, Fp1/Fp2–O1/O2, and C3/C4–O1/O2. The factor band included frequency bands δ, θ, α, σ, β, and γ. Multiple comparison procedure (t-tests) with the Bonferroni correction was performed if ANOVA revealed significant effect of one of the three factors.

Pearson's correlation coefficient ρ was used to indicate the dependence between measures.

2.6. *Software*

Data analysis and statistics was performed by functions and scripts developed in software package Matlab (The Math Works Inc., USA) and the permutation surrogate data were created with the INTERACT Toolbox (http://ndw.cs.cas.cz/software).

3. Results

3.1. *Comparison of coherence and MPC z-score*

3.1.1. *Statistical differences between pairs of vigilance states*

Figures 1 and 2 show the mean values and standard deviations of MPC z-score and coherence, respectively, computed from all subjects and Table 1 includes the results of statistical comparison between pairs of vigilance stages wakefulness, nonREM sleep and REM sleep.

Z-score and coherence showed the same significant differences between pairs of sleep stages and wakefulness in 104 from all 126 tests. In 20 cases there were non-contradictory differences, i.e. a significant difference shown by one measure was not significantly different by the second measure (comparison wakefulness/nonREM sleep: alpha Fp1/Fp2–O1/O2 and C3/O1–C4/O2, sigma Fp1/C3–C4/O2 and C3/O1–Fp2/C4, gamma Fp1/C3–C4/O2; comparison wakefulness/REM sleep: delta Fp1/Fp2–C3/C4, Fp1/Fp2–O1/O2, and C3/C4–O1/O2, theta Fp1/Fp2–O1/O2, C3/C4–O1/O2, and C3/O1–Fp2/C4, alpha C3/O1–C4/O2, sigma Fp1/Fp2–O1/O2 and beta Fp1/Fp2–O1/O2; comparison nonREM/REM sleep: delta Fp1/C3–C4/O2, C3/O1–Fp2/C4, theta Fp1/C3–C4/O2, alpha C3/C4–O1/O2, sigma C3/O1–Fp2/C4, and gamma C3/C4–O1/O2). The measures demonstrated opposite behaviour in two cases only – comparison of nonREM and REM sleep in sigma band at Fp1/C3–C4/O2 (coherence was lower in REM sleep than in nonREM sleep and z-score vice versa) and the comparison of wakefulness and REM sleep in beta band at C3/C4–O1/O2 (coherence was lower in REM sleep than in wakefulness and z-score was higher in REM sleep).

						coh			MPC z-score			ρ_A		
ρ(z, ρ_A)	fr.band	channels	μ(coh)	μ(MPC z-score)	$\mu(\rho_A)$	W-N	W-R	N-R	W-N	W-R	N-R	W-N	W-R	N-R
0.684	theta	C3/O1-C4/O2	0.584	22.323	0.626	+	+	n.s.	+	+	n.s.	+	+	-
0.678	sigma	Fp1/C3-Fp2/C4	0.387	24.538	0.558	+	+	-	+	+	-	+	+	-
0.677	theta	Fp1/C3-Fp2/C4	0.529	20.241	0.591	+	+	+	+	+	+	n.s.	+	+
0.674	beta	Fp1/C3-Fp2/C4	0.243	24.230	0.330	+	+	+	+	+	+	+	+	+
0.664	beta	C3/O1-C4/O2	0.296	28.299	0.370	+	+	+	+	+	+	+	+	+
0.642	alpha	C3/O1-C4/O2	0.510	25.773	0.581	-	-	+	n.s.	n.s.	+	-	-	+
0.621	alpha	Fp1/C3-Fp2/C4	0.451	23.395	0.549	+	+	-	+	+	-	+	+	-
0.587	sigma	C3/O1-C4/O2	0.386	26.139	0.501	+	+	+	+	+	+	+	+	⊖
0.542	delta	C3/O1-C4/O2	0.608	12.690	0.645	+	+	+	+	+	+	+	+	+
0.532	gamma	Fp1/C3-Fp2/C4	0.176	25.513	0.266	+	+	+	+	+	+	⊖	+	+
0.489	gamma	C3/O1-C4/O2	0.211	30.113	0.270	+	+	+	+	+	+	⊖	n.s.	+
0.479	beta	C3/C4-O1/O2	0.197	21.943	0.245	+	+	-	+	⊖	-	⊖	-	-
0.472	delta	Fp1/C3-Fp2/C4	0.706	13.639	0.746	+	+	+	+	+	+	⊖	n.s.	+
0.464	sigma	Fp1/Fp2-C3/C4	0.254	11.427	0.360	+	+	-	+	+	-	+	n.s.	-
0.445	alpha	C3/C4-O1/O2	0.262	15.429	0.313	n.s.	n.s.	n.s.	n.s.	n.s.	+	-	-	+
0.441	theta	Fp1/Fp2-C3/C4	0.332	9.843	0.405	+	n.s.	-	+	n.s.	-	+	-	-
0.440	theta	C3/C4-O1/O2	0.257	12.036	0.297	+	-	-	+	n.s.	-	⊖	-	-
0.436	alpha	Fp1/Fp2-C3/C4	0.321	10.370	0.383	+	n.s.	-	+	n.s.	-	+	-	-
0.422	sigma	C3/C4-O1/O2	0.246	18.790	0.358	+	n.s.	-	+	n.s.	-	+	n.s.	-
0.410	beta	Fp1/Fp2-C3/C4	0.131	13.036	0.194	+	+	+	+	+	+	n.s.	+	+
0.403	gamma	Fp1/Fp2-O1/O2	0.103	12.096	0.133	+	+	-	+	+	-	⊖	⊖	n.s.
0.402	gamma	C3/C4-O1/O2	0.196	26.195	0.218	+	+	n.s.	+	+	+	⊖	⊖	n.s.
0.366	gamma	Fp1/Fp2-C3/C4	0.134	14.973	0.177	+	+	+	+	+	+	⊖	⊖	+
0.304	delta	Fp1/Fp2-C3/C4	0.360	5.864	0.444	+	+	-	+	n.s.	-	+	⊖	-
0.290	delta	C3/C4-O1/O2	0.250	5.994	0.307	+	-	-	+	n.s.	-	⊖	-	-
0.275	theta	Fp1/Fp2-O1/O2	0.085	4.379	0.134	+	-	-	+	n.s.	-	⊖	-	-
0.259	theta	C3/O1-Fp2/C4	0.062	4.448	0.165	-	-	n.s.	-	n.s.	n.s.	-	-	n.s.
0.252	alpha	C3/O1-Fp2/C4	0.081	6.710	0.234	-	-	+	-	-	+	-	-	⊖
0.240	gamma	Fp1/C3-C4/O2	0.028	6.960	0.117	n.s.	+	+	+	+	+	⊖	⊖	+
0.237	gamma	C3/O1-Fp2/C4	0.034	8.363	0.121	+	+	+	+	+	+	⊖	⊖	+
0.236	sigma	Fp1/Fp2-O1/O2	0.067	6.021	0.181	+	n.s.	-	+	+	-	+	⊖	-
0.216	alpha	Fp1/Fp2-O1/O2	0.084	5.552	0.133	n.s.	n.s.	-	+	n.s.	-	⊖	-	-
0.205	beta	C3/O1-Fp2/C4	0.035	6.713	0.152	+	+	n.s.	+	+	n.s.	n.s.	+	n.s.
0.190	delta	C3/O1-Fp2/C4	0.106	2.364	0.260	-	-	n.s.	-	-	+	-	-	⊖
0.188	delta	Fp1/Fp2-O1/O2	0.102	2.227	0.178	+	-	-	+	n.s.	-	⊖	-	-
0.182	theta	Fp1/C3-C4/O2	0.047	3.409	0.150	-	-	n.s.	-	-	+	-	-	n.s.
0.181	beta	Fp1/Fp2-O1/O2	0.044	6.359	0.104	+	n.s.	-	+	+	-	⊖	⊖	n.s.
0.174	alpha	Fp1/C3-C4/O2	0.066	5.567	0.221	-	-	+	-	-	+	n.s.	-	⊖
0.165	sigma	C3/O1-Fp2/C4	0.066	6.723	0.303	n.s.	n.s.	n.s.	-	n.s.	+	⊕	n.s.	⊖
0.150	delta	Fp1/C3-C4/O2	0.094	2.020	0.250	-	-	n.s.	-	-	+	-	-	⊖
0.124	beta	Fp1/C3-C4/O2	0.024	4.969	0.141	n.s.	n.s.	n.s.	n.s.	n.s.	n.s.	n.s.	n.s.	n.s.
0.122	sigma	Fp1/C3-C4/O2	0.054	5.271	0.289	n.s.	-	-	-	-	⊕	⊕	n.s.	⊖

Table 1

Comparison of correlation coefficients between amplitude correlations and phase synchronization ρ(z, ρ_A), mean coherence μ(coh), mean values of MPC z-score μ(MPC z-score), and mean correlations between amplitudes $\mu(\rho_A)$. The results are sorted according to ρ(z, ρ_A) (1st column) in descending order. There are also the results of statistical tests between vigilance stages wakefulness (W), nonREM sleep (N) and REM sleep (R). + (-) means significantly higher (lower) mean in the second stage in comparison with the first one; n.s. means no significant difference. The signs ⊖, ⊕ mark contradictory significant differences. P-value < 0.05, multiple comparison procedure (t-tests) with the Bonferroni correction.

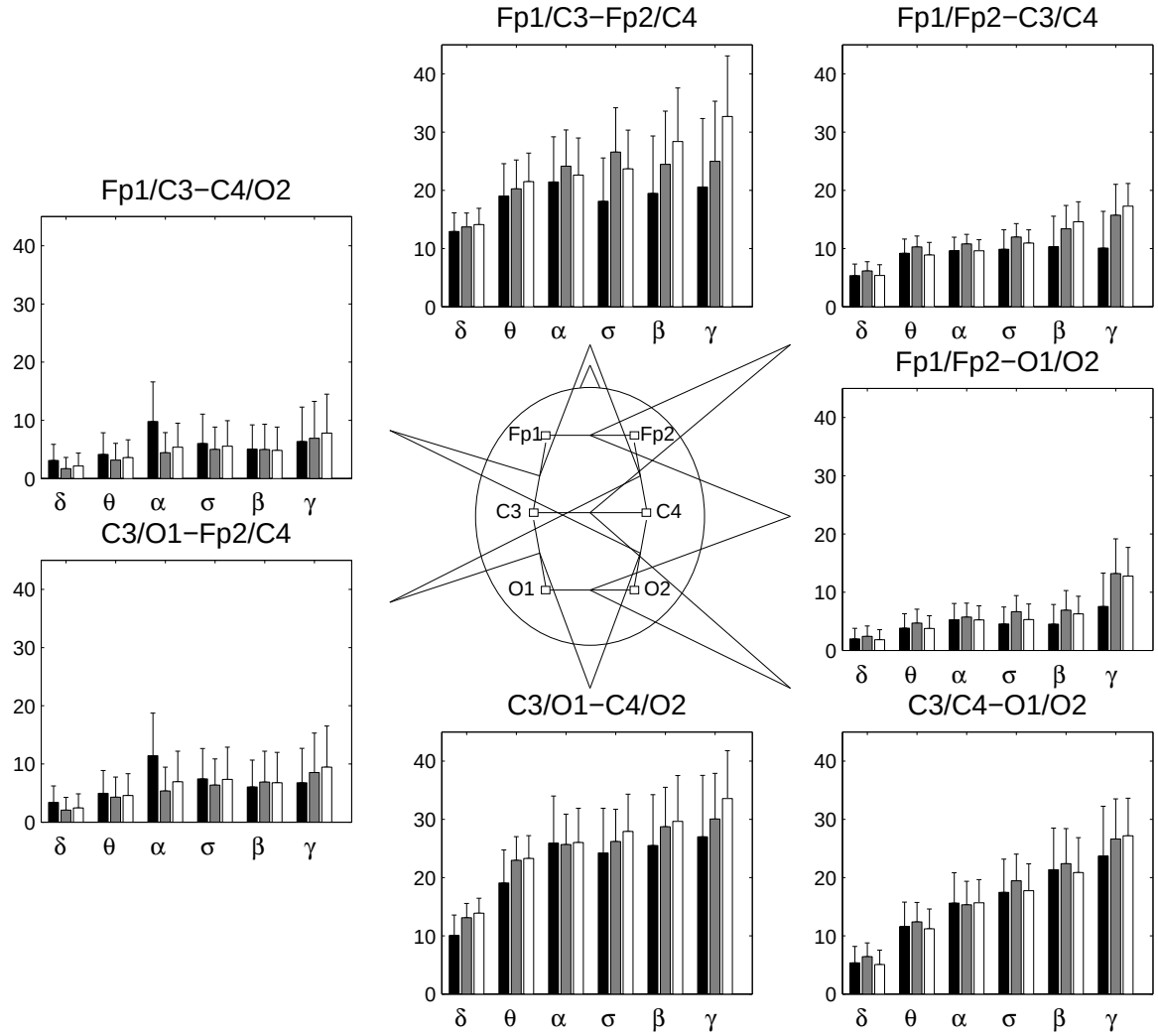

Fig. 1. All subjects' mean values (bars) and standard deviations (whiskers) of MPC z-score in wakefulness (black bars), nonREM sleep (grey bars) and REM sleep (white bars). Note that the apparent increase of the MPC z-scores with the increasing frequency is discussed in Sec. 3.1.2.

3.1.2. *Dependence on frequency*

When comparing the stage-independent behaviour of both measures, coherence showed the tendency to decrease or to be constant in the dependence on the frequency (Figure 2); in contrast to MPC z-score, which had the tendency to increase with the frequency (Figure 1). The decreasing behaviour of coherence across frequency is in accordance with the literature (Achermann and Borbély, 1998a). A potential reason for the increasing tendency of z-scores could be the various numbers of phase cycles in the 30 sec long segment. The higher the frequency the more phase cycles are in the segments of the same length; e. g. in the delta band there are on average 60 phase cycles with the mean frequency 2 Hz in the 30s long segment, however, in the gamma band with the mean frequency 35 Hz the number of phase cycles is above 1000.

In order to analyze whether the tendency of MPC z-score to increase with frequency is due to the various numbers of phase cycles for different frequency bands in a 30s window, the length of the segments was adjusted to achieve similar numbers of cycles per segment. In addition signals were subsampled for various frequencies differently to achieve similar numbers of points per cycle. With parameters listed in Table 2 approximately 60 phase cycles per segment and 9 points per cycle were obtained.

Figure 3 contrasts the dependence of the MPC z-score on the frequency when it is computed for the same

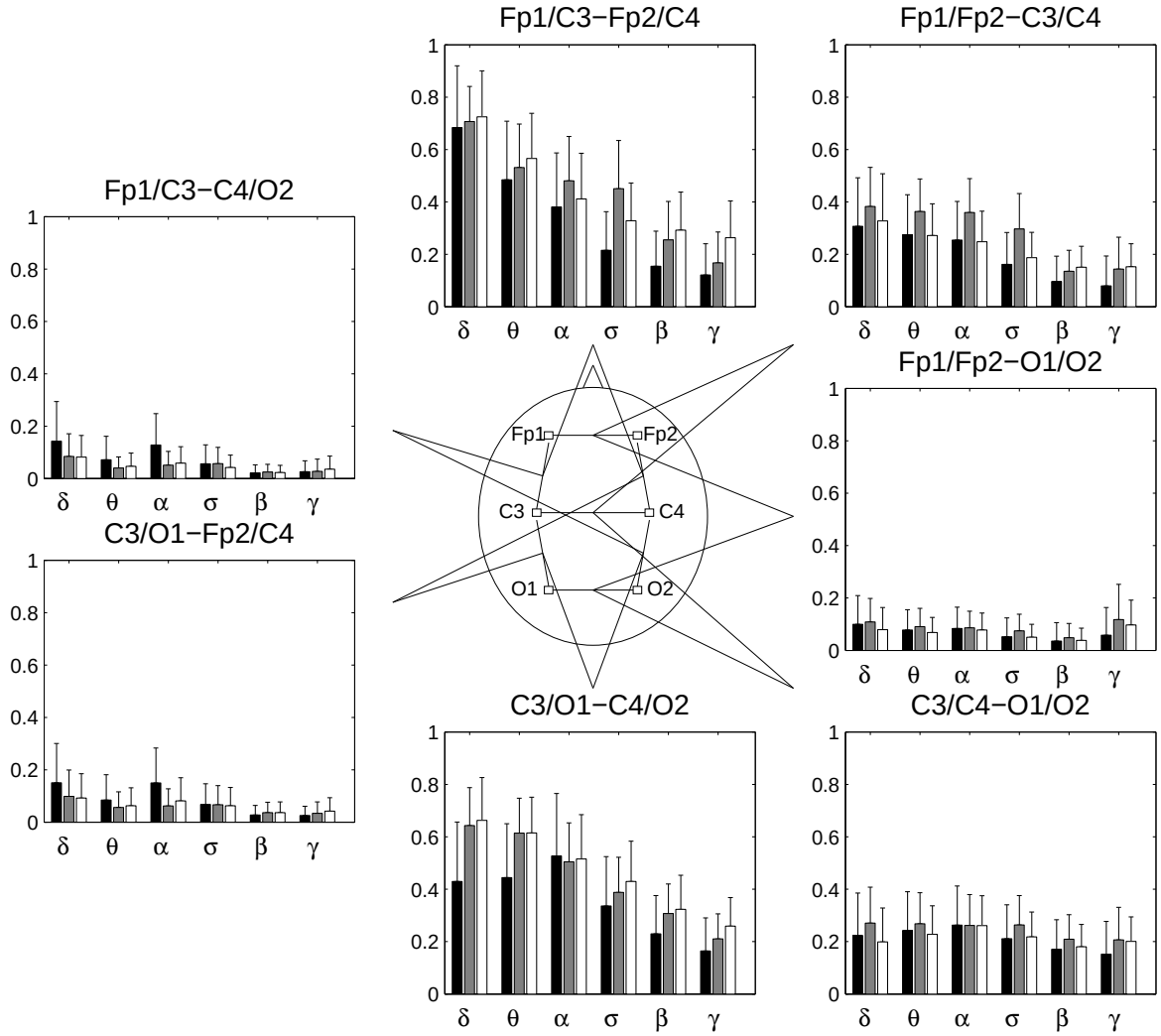

Fig. 2. All subjects' mean values (bars) and standard deviations (whiskers) of coherence in wakefulness (black bars), nonREM sleep (grey bars) and REM sleep (white bars).

length of segments (30 sec.) with when it is computed for approximately the same numbers of phase cycles per segment. Mean values over all subjects and sleep stages of MPC z-score computed for approximately the same numbers of phase cycles showed decreasing behaviour with the frequency, similar to the coherence. From the topological point of view the most evident difference can be seen for interhemispheric homologous derivations (Fp1/C3–Fp2/C4, C3/O1–C4/O2).

The effect of the various numbers of phase cycles on the mean phase coherence R is illustrated in Figure 4, where the results computed for one entire night with both values of parameters for sigma band are compared. R computed from more phase cycles achieved more stable values, so the variance of the results was lower (for both signals – EEG and permutation surrogate data). In addition, permutation surrogate data computed from more phase cycles achieved a better level of randomization and their overall mean was lower. As a consequence of lower mean values and standard deviations of permutation surrogate data, the MPC z-score was higher.

3.1.3. *Correlation of phase synchronization and coherence*

Correlation coefficient between MPC z-score and coherence can be found in Table 3. The values ranged from 0.47 to 0.89 with the highest values achieved between hemispheres at homologous positions (Fp1/C3–

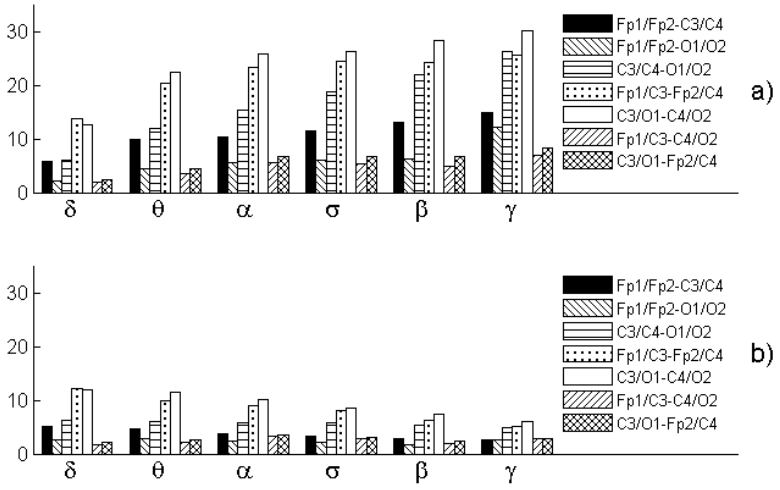

Fig. 3. Dependence of MPC z-score on frequency: a) Mean values of MPC z-score over all subjects and sleep stages computed for 30s long segments and increasing number of phase cycles with frequency band. b) Mean values of MPC z-score over all subjects and sleep stages computed for various lengths of the segments but approximately the same numbers of the phase cycles at each frequency band, using the parameters given in Tab. 2.

	delta	theta	alpha	sigma	beta	gamma
mean frequency [Hz]	2	6	10	14	22	35
spectral width [Hz]	1	2	2	3	7	7
sampling frequency [Hz]	16	51.2	85.3	128	256	256
segment length [s]	30	10	6	4.3	2.8	1.8

Table 2
Parameters of MPC z-score calculation with keeping approximately the same number of cycles and samples for each frequency band, used to test the frequency dependence of the MPC z-score.

Fp2/C4, C3/O1–C4/O2), where also the MPC z-score and coherence achieved the highest values.

3.2. *Phase vs. complete synchronization*

Figure 5 displays mean values and standard deviations of correlation coefficient ρ_A between the analytical amplitudes computed for all frequency bands and for the vigilance stages. To investigate whether complete or phase synchronization occurs, the correlation coefficient $\rho(z, \rho_A)$ between ρ_A and the MPC z-score was calculated. Table 1 contains the results sorted according to $\rho(z, \rho_A)$ in descending order together with a comparison of statistical differences of all three measures between vigilance stages wakefulness, nonREM sleep and REM sleep. For values of $\rho(z, \rho_A)$ higher than 0.5 both ρ_A and MPC z-scores demonstrated the same significant statistical differences between vigilance stages; with the decreasing values of $\rho(z, \rho_A)$ the results of statistical tests using ρ_A and MPC z-score began to disagree. From the topographical point of view the highest values of $\rho(z, \rho_A)$ were achieved between homologous positions between hemispheres; conversely, the lowest values of $\rho(z, \rho_A)$ occurred mostly between nonhomologous positions between hemispheres and between fronto-occipital positions Fp1/Fp2-O1/O2. Regarding the dependence of $\rho(z, \rho_A)$ on frequency, there was no apparent relationship.

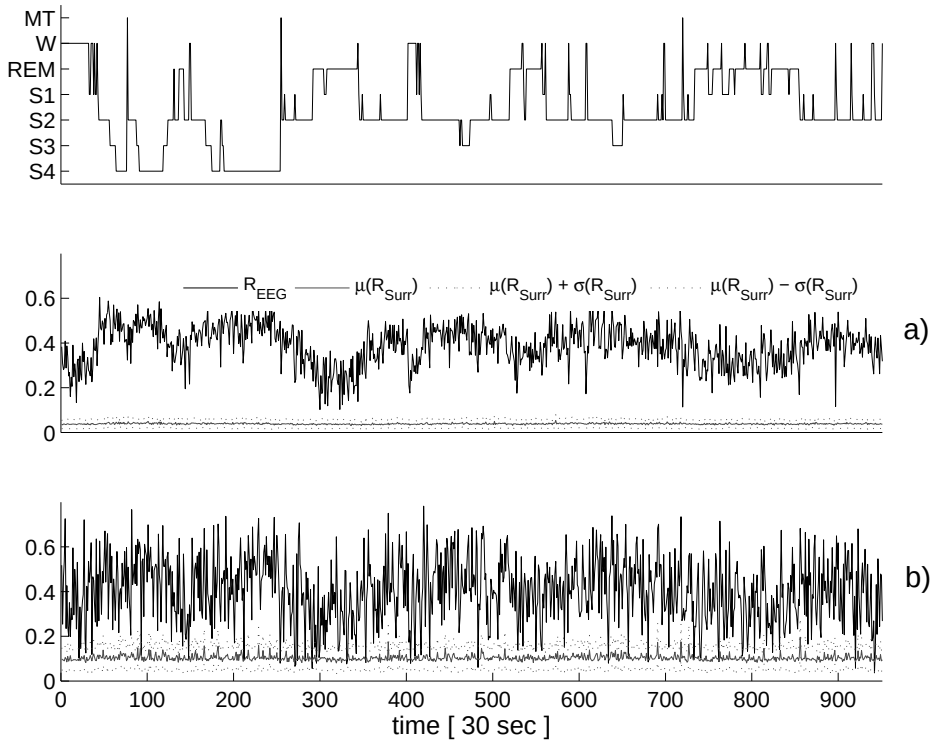

Fig. 4. Example of mean phase coherence R computed for original data and surrogate data for different numbers of phase cycles, sigma band, C3/C4-O1/O2 derivations. a) R computed using 30s long segments ($\approx$ 420 phase cycles), 256 Hz sampling frequency ($\approx$ 18 points per cycle). b) R computed using 4.3s long segments ($\approx$ 60 phase cycles), 128 Hz (9 points per cycle). Black line: original EEG data, grey full line: mean values of surrogate data, grey dotted line: mean values $\pm$ standard deviations of surrogate data
Abbreviations: MT - movement time, W - wakefulness, S1–S4 - stages of nonREM sleep.

	delta	theta	alpha	sigma	beta	gamma
Fp1/Fp2-C3/C4	0.62	0.68	0.65	0.67	0.75	0.79
Fp1/Fp2-O1/O2	0.51	0.63	0.59	0.59	0.62	0.81
C3/C4-O1/O2	0.64	0.72	0.68	0.70	0.74	0.72
Fp1/C3-Fp2/C4	0.63	0.80	0.81	0.83	0.85	0.85
C3/O1-C4/O2	0.72	0.77	0.78	0.75	0.77	0.78
Fp1/C3-C4/O2	0.47	0.58	0.65	0.58	0.60	0.73
C3/O1-Fp2/C4	0.53	0.66	0.72	0.63	0.70	0.76

Table 3
Correlation coefficient between values of MPC z-score and coherence.

4. Discussion

4.1. *Comparison of coherence and MPC z-score*

In previous studies concerning coherence of EEG during sleep (Dumermuth and Lehmann, 1981; Dumermuth et al., 1983; Achermann and Borbély, 1998a,b; Duckrow and Zaveri, 2005) only the coherence spectra were investigated. In this study the band-averaged coherence (Andrew and Pfurtscheller, 1996) was computed in order to directly compare the coherence results with the phase synchronization measure MPC z-score.

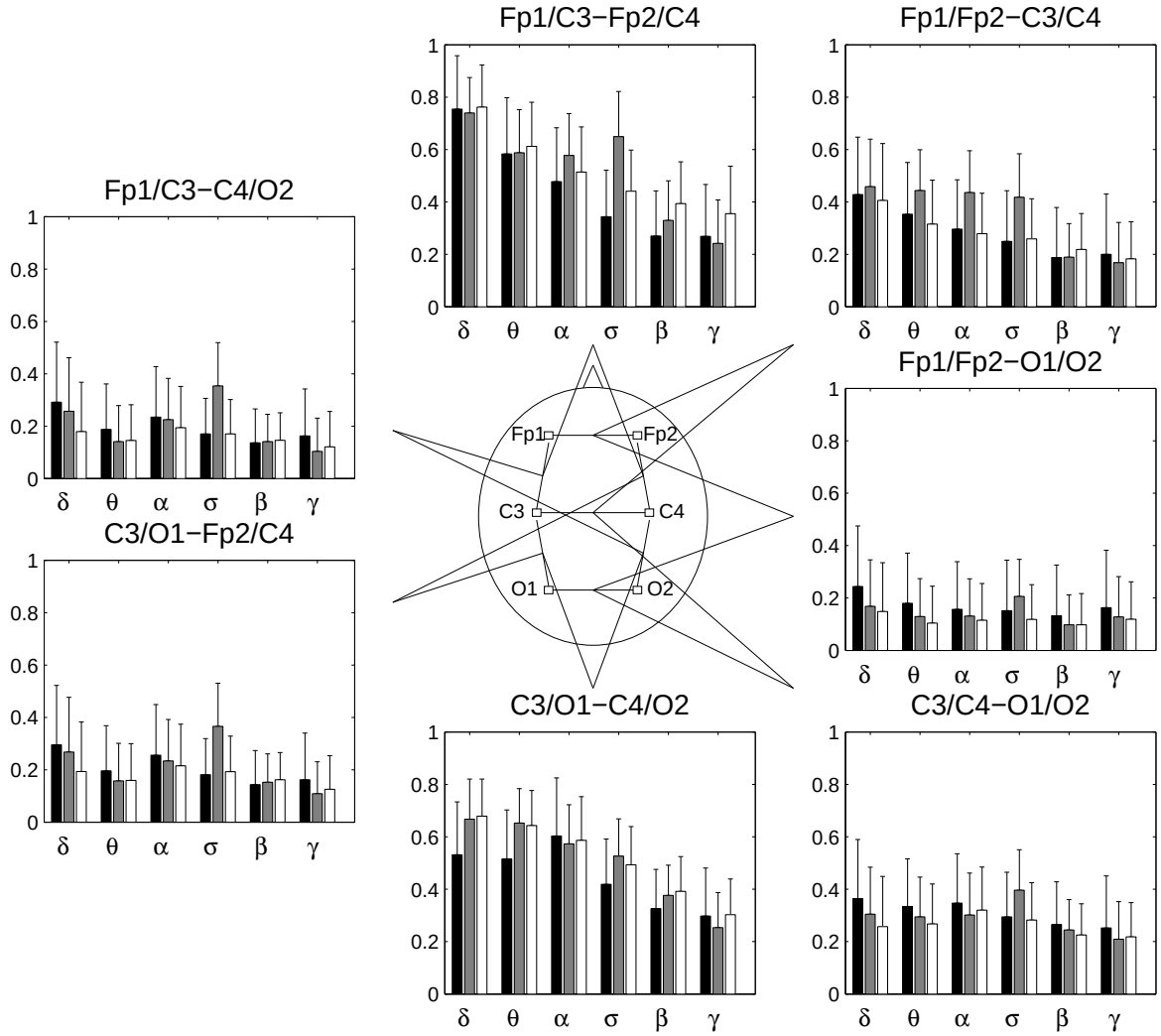

Fig. 5. All subjects' mean values (bars) and standard deviations (whiskers) of correlation coefficient of amplitudes in wakefulness (black bars), nonREM sleep (grey bars) and REM sleep (white bars).

However, the results regarding coherence in general were consistent with the works based on the bipolar electrode derivations (Achermann and Borbély, 1998a,b): coherence between interhemispheric homologous derivations (Fp1/C3–Fp2/C4, C3/O1–C4/O2) was highest in the low frequency bands for all stages and showed a declining tendency from low to high frequencies; coherence between all other pairs of derivations showed flat, low-level values. Coherence between Fp1/C3-Fp2/C4 in alpha and sigma bands was higher during NREM sleep than during REM sleep and vice versa in the higher - beta and gamma - frequency bands. Coherence between C3/O1-C4/O2 was slightly higher during REM sleep than during NREM sleep in all frequency bands except the theta band. In contrast to Achermann and Borbély (1998b), coherence between Fp1/C3-Fp2/C4 in the delta band was higher during REM sleep than during NREM sleep. This difference probably arose because the lowest frequencies (below 1 Hz) were excluded from our analysis or because the derivations of the signals were slightly different – F3/C3-F4/C4 in (Achermann and Borbély, 1998b).

The first objective of this study was to compare coherence and phase synchronization in the human sleep EEG. Analysis was done in two ways - investigation of sleep stage differences and the dependence on frequency. Most of the statistical tests demonstrated the same or non-contradictory results; the two cases where coherence and MPC z-score showed opposite behaviour corresponded to low values of coherence. The stage-independent tendency of MPC z-score to increase with the frequency was the consequence of various

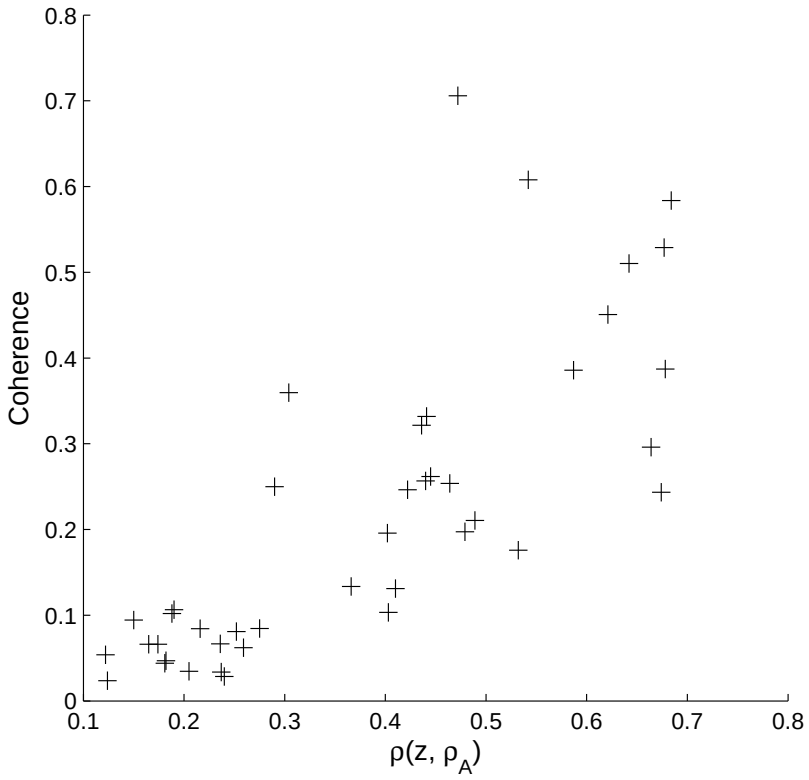

Fig. 6. Dependence between mean values of coherence (over all states) and correlation coefficients between amplitude correlations and phase synchronization $\rho(z, \rho_A)$. Mean values of coherence and $\rho(z, \rho_A)$ are listed in Table 1.

numbers of the phase cycles used in calculation in each frequency band. After adjusting the numbers of phase cycles to approximately the same value, MPC z-score showed the same behaviour as coherence. From these findings it can be concluded that coherence and phase synchronization provide essentially the same information and both measures can be used interchangeably.

4.2. *Phase vs. complete synchronization*

The second objective of this study was to apply the theory of synchronization between two nonlinear, possibly chaotic oscillators and to investigate what type of synchronization occurs during various sleep stages. In models, the type of synchronization changes with increasing value of coupling between the oscillators, from the uncorrelated state when the coupling is zero through phase synchronization when the coupling is weak, to complete synchronization when the coupling exceeds a certain level (Osipov et al., 2003).

High values of the correlation coefficient $\rho(z, \rho_A)$ between MPC z-score and amplitude correlations ρ_A can be considered as an indicator of complete synchronization. $\rho(z, \rho_A)$ reflects coincidental behaviour of both measures - with increasing phase synchronization also the amplitude correlation increases, and vice versa. Complete synchronization is manifested by highly coherent phases and dependent amplitudes. In such situations, spectral coherence is also high since it is influenced by both phases and amplitudes of spectra (see Figure 6). If we consider all spectral bands, but the gamma band, the signs of complete synchronization can be seen in interhemispheric homologous derivations Fp1/C3–Fp2/C4, C3/O1–C4/O2 which are characterized by values of $\rho(z, \rho_A)$ close to, or greater than 0.5, see Tab. 1.

With decreasing values of $\rho(z, \rho_A)$ the stages with the emphasis shifted to phase synchronization emerged. We can observe the decrease of $\rho(z, \rho_A)$ under 0.5 for the derivations Fp1/Fp2–C3/C4, Fp1/Fp2–O1/O2, and

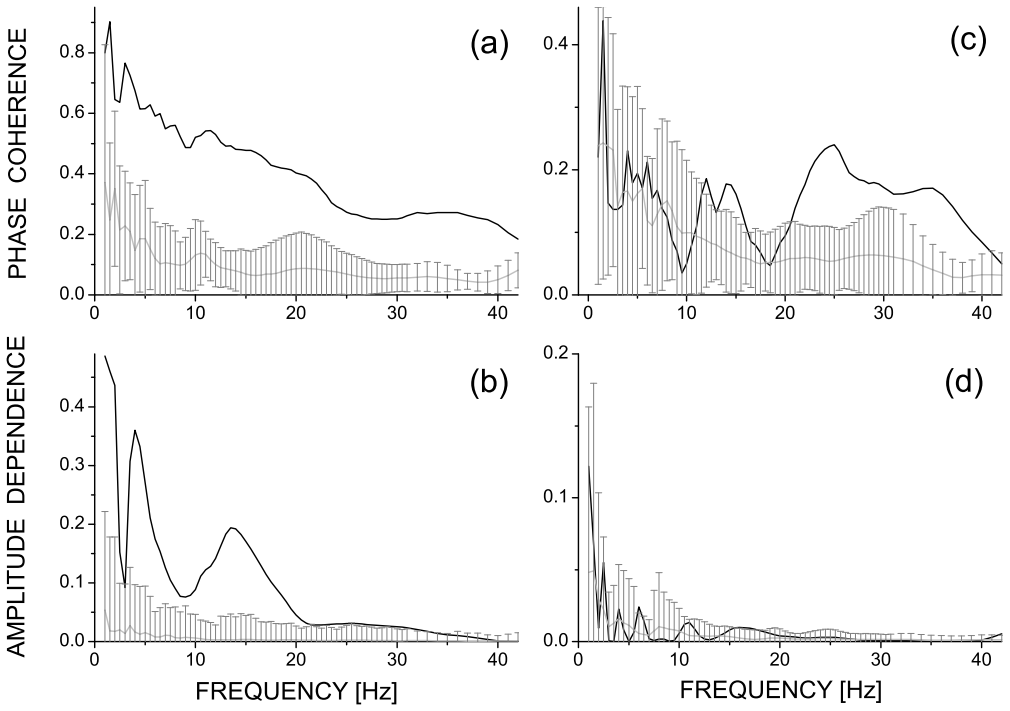

Fig. 7. Mean phase coherence spectra (a, c; solid black lines) and analytic amplitude dependence spectra (b, d; solid black lines) for the interhemispheric homologous derivations Fp1/C3–Fp2/C4 (a, b) and the interhemispheric nonhomologous derivations C3/O1–Fp2/C4 (c, d) for an EEG segment of non-REM sleep. The gray lines illustrate mean values for surrogate data representing null hypothesis of independence, the grey bars give the surrogate mean±2SD range.

C3/C4–O1/O2 and occasional discrepancies occur between the MPC z-score and the spectral coherence on one side and the amplitude correlations ρ_A on the other side. Finally, the interhemispheric nonhomologous derivations Fp1/C3–C4/O2, C3/O1–Fp2/C4 give the $\rho(z, \rho_A)$ values close to, or smaller than 0.2. Their amplitude correlations ρ_A are also small ($\lessapprox 0.2$) and change (with respect to sleep stages) independently from the other two measures. The spectral coherence falls below 0.1, however, even the low values of coherence reflect the same changes between the vigilance/sleep states as the MPC z-scores. Phase synchronization (phase coherence) is apparently the principal mechanism of coordination between cortical areas, however, can be equally well characterized by the spectral coherence and the MPC z-scores, the two measures based on different physical concepts.

From the above description one can conclude that the type of synchronization depends on topographic positions of considered electrodes. This conclusion, however, does not hold for the gamma band. In the gamma band we can see contradictory differences between the wake state W and the sleep states (N and R) irrespectively of $\rho(z, \rho_A)$ values (see Tab. 1). On the other hand, the amplitude correlations ρ_A changes between REM and non-REM sleep stages in accord with changes of the measures of phase coherence. All considered synchrony measures attain greater values in REM stages.

For better understanding of the observed synchronization phenomena, in Figs. 7 and 8 we present mean phase coherence spectra (Figs. 7a, c and 8a, c) and amplitude dependence spectra (Figs. 7b, d and 8b, d) for the interhemispheric homologous derivations Fp1/C3–Fp2/C4 (Figs. 7a, b and 8a, b) and the interhemispheric nonhomologous derivations C3/O1–Fp2/C4 (Figs. 7c, d and 8c, d) for a segment of the non-REM sleep state (Fig. 7) and a segment of the REM sleep state (Fig. 8). Unlike in the above statistical analyses,

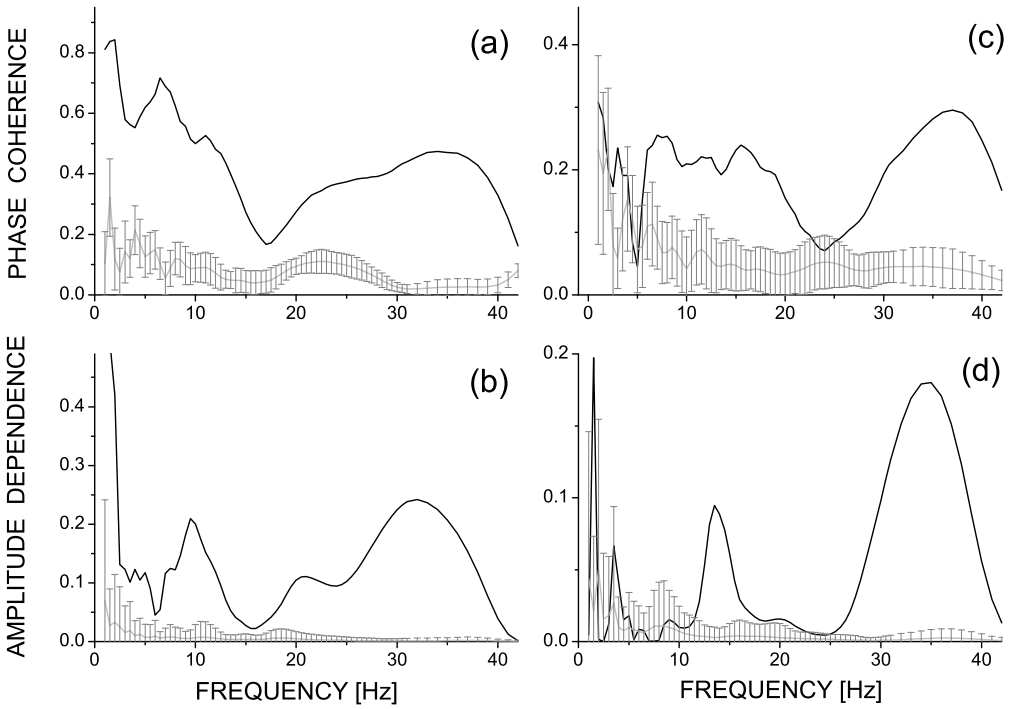

Fig. 8. Mean phase coherence spectra (a, c; solid black lines) and analytic amplitude dependence spectra (b, d; solid black lines) for the interhemispheric homologous derivations Fp1/C3–Fp2/C4 (a, b) and the interhemispheric nonhomologous derivations C3/O1–Fp2/C4 (c, d) for an EEG segment of REM sleep. The gray lines illustrate mean values for surrogate data representing null hypothesis of independence, the grey bars give the surrogate mean±2SD range.

here we used a large number (70) of central wavelet frequencies for which MPC and analytic amplitude dependence have been computed. The results form seemingly continuous spectra, illustrated by the solid black lines in Figs. 7 and 8. The grey lines illustrate mean values for surrogate data representing null hypothesis of independence; the grey bars located at each wavelet central frequency show the range mean±2SD (standard deviations) of the surrogate data. The plotted amplitude dependence is the amplitude correlation coefficient c transformed as -0.5log$(1 - c^2)$ (Paluš, 1995).

In the non-REM state (Fig. 7), similarly as in the vigilant state (not shown), for the derivations Fp1/C3–Fp2/C4 (Figs. 7a, b) we can see complete synchronization (significant both MPC and amplitude dependence) in all, but the gamma band. In the gamma band, only phase synchronization is present. In the case of the derivations C3/O1–Fp2/C4 there is no amplitude dependence at all (Fig. 7d, the data values lie within the surrogate range), while significant mean phase coherence is present in a narrow sigma band and in a wider beta and gamma band (Fig. 7c). Significant phase coherence can occur in other spectral bands in other data segments of this type.

In the REM state complete synchronization extends over the whole studied spectral range in the case of the derivations Fp1/C3–Fp2/C4 (Fig. 8a, b). In the derivations C3/O1–Fp2/C4, the significant mean phase coherence spreads over the theta, alpha, sigma, a part of beta, and the gamma bands (Fig. 8c). The amplitude dependence (Fig. 8d) results in complete synchronization in sigma and, more typically, in the gamma band.

Based on the results summary in Tab. 1 and the illustrative examples in Figs. 7 and 8 we understand that unlike in the other spectral bands, the type of synchronization in the gamma band does not depend

on topography, but on sleep state. The wake state and the non-REM sleep state are dominated by phase synchronization, while the REM sleep state is characterized by complete synchronization.

5. Conclusion

Using whole-night EEG recordings from 25 healthy subjects we quantified sleep stage-related differences in coupling between EEG signals from different scalp locations. Traditional analysis using the spectral coherence measure confirmed the results of previous studies (Dumermuth and Lehmann, 1981; Dumermuth et al., 1983; Achermann and Borbély, 1998a; Duckrow and Zaveri, 2005). Phase synchronization analysis allowed us to separate the effect of phase and amplitude on the coordination between different areas of the cortex. Phase synchronization was quantified by using mean phase coherence (MPC) and tested with z-score statistics using an ensemble of permutation surrogate data. Pearson's correlation coefficient was used to estimate correlations between the instantaneous amplitudes. High correlation between the two measures indicated states of complete synchronization when both measures gave results consistent with the coherence analysis. With decreasing correlations between the MPC z-score and the amplitude correlations, the latter started to differ from the MPC z-score and coherence in respect to coupling differences between vigilance/sleep stages. Specifically the coordination between the cortical areas was weaker, dominated by phase synchronization. Coherence and MPC z-score, however, demonstrated practically the same statistical differences between vigilance stages.

In spite of recent claims, e.g. Lachaux et al. (1999), phase synchronization analysis is not superior to the coherence analysis in that both techniques lead to equivalent results. The coupling between EEG signals from different cortical areas is dominated by phase synchronization which turns into complete synchronization in the most strongly coupled EEG signals. Considering gamma band, phase synchronization during vigilance and non-REM sleep turns into complete synchronization in REM sleep stages, while in other spectral bands the type of synchronization depends on topographic positions of considered electrodes.

Acknowledgements

The authors would like to acknowledge the Siesta Group Schlafanalyse GmbH as the source of the sleep EEG and thank them, particularly G. Dorffner, for making their data available. The authors would also like to thank P. Janata and M. Vejmelka for valuable discussions and critical remarks.

This work has been supported by the EC FP7 project BrainSync (EC: HEALTH-F2-2008-200728, CR: MSM/7E08027); and in part by the Slovak Grant Agency for Science (grant No 2/0019/10) and the bilateral project "Modern Methods for Analysis of Electrophysiological Signals" of the Slovak Academy of Sciences and the Academy of Sciences of the Czech Republic.

References

Achermann, P., Borbély, A. A., 1998a. Coherence analysis of the human sleep electroencephalogram. Neuroscience 85, 1195–1208.

Achermann, P., Borbély, A. A., 1998b. Temporal evolution of coherence and power in the human sleep electroencephalogram. J Sleep Res 7, 36–41.

Anderer, P., Gruber, G., Parapatics, S., Woertz, M., Miazhynskaia, T., Klösch, G. et al., 2005. An E-Health Solution for Automatic Sleep Classification according to Rechtschaffen and Kales: Validation Study of the Somnolyzer 24 x 7 Utilizing the Siesta Database. Neuropsychobiology 51 (3), 115–133.

Andrew, C., Pfurtscheller, G., 1996. Event-related coherence as a tool for studying dynamic interaction of brain regions. Electroencephalogr Clin Neurophysiol 98 (2), 144–148.

Angelini, L., Tommaso, M. D., Guido, M., Hu, K., Ivanov, P. C., Marinazzo, D. et al., 2004. Steady-state visual evoked potentials and phase synchronization in migraine patients. Phys Rev Lett 93 (3), 038103.

Bhattacharya, J., Petsche, H., Feldmann, U., Rescher, B., 2001. EEG gamma-band phase synchronization between posterior and frontal cortex during mental rotation in humans. Neurosci Lett 311 (1), 29–32.

Bob, P., Paluš, M., Šusta, M., Glaslová, K., 2008. EEG phase synchronization in patients with paranoid schizophrenia. Neurosci Lett 447 (1), 73 – 77.

Duckrow, R. B., Zaveri, H. P., 2005. Coherence of the electroencephalogram during the first sleep cycle. Clin Neurophysiol 116, 1088–1095.

Dumermuth, G., Lange, B., Lehmann, D., Meier, C. A., Dinkelmann, R., Molinari, L., 1983. Spectral Analysis of All-Nigth Sleep EEG in Healthy Adults. Eur Neurol 22 (5), 322–339.

Dumermuth, G., Lehmann, D., 1981. EEG Power and Coherence during Non-REM and REM Phases in Humans in All-Night Sleep Analyses. Eur Neurol 20 (6), 429–434.

Fein, G., Raz, J., Brown, F. F., Merrin, E. L., 1988. Common reference coherence data are confounded by power and phase effects. Electroencephalogr Clin Neurophysiol 69 (6), 581–584.

Fries, P., 2009. Neuronal gamma-band synchronization as a fundamental process in cortical computation. Annu Rev Neurosci 32, 209–224.

Gabor, D., 1946. Theory of communication. J IEE London 93, 429–457.

Galka, A., 2000. Topics in Nonlinear Time Series Analysis. World Scientific.

Gray, C. M., König, P., Engel, A. K., Singer, W., 1989. Oscillatory responses in cat visual cortex exhibit inter-columnar synchronization which reflects global stimulus properties. Nature 338, 334–337.

Lachaux, J.-P., Rodriguez, E., Martinerie, J., Varela, F. J., 1999. Measuring phase synchrony in brain signals. Hum Brain Mapp 8 (4), 194–208.

Le Van Quyen, M., Foucher, J., J.-P., L., Rodriguez, E., Lutz, A., Martinerie, J., Varela, F. J., 2001. Comparison of Hilbert transform and wavelet methods for the analysis of neuronal synchrony. J Neurosci Methods 111 (2), 83–98.

Mormann, F., Lehnertz, K., David, P., Elger, C. E., 2000. Mean phase coherence as a measure for phase synchronization and its application to the EEG of epilepsy patients. Physica D 144 (3-4), 358–369.

Nunez, P. L., Srinivasan, R., Westdorp, A. F., Wijesinghe, R. S., Tucker, D. M., Silberstein, R. B. et al., 1997. EEG coherency I: statistics, reference electrode, volume conduction, Laplacians, cortical imaging, and interpretation at multiple scales. Electroencephalogr Clin Neurophysiol 103 (5), 499–515.

Osipov, G. V., Hu, B., Zhou, C., Ivanchenko, M. V., J., K., 2003. Three types of transitions to phase synchronization in coupled chaotic oscillators. Phys Rev Lett 91, 024101.

Paluš, M., 1995. Testing for nonlinearity using redundancies: quantitative and qualitative aspects. Physica D 80 (1-2), 186–205.

Paluš, M., Novotná, D., Tichavský, P., 2005. Shifts of seasons at the European mid-latitudes: Natural fluctuations correlated with the North Atlantic Oscillation. Geophys Res Lett 32, L12805.

Rappelsberger, P., 2000. EEG coherence analysis: a method to visualise functional connections. In: Bernd, S., Krijzer, F., Ferber, G., Anderer, P. (Eds.), Electrophysiological Brain Research in Preclinical and Clinical Pharmacology and Related Fields. Facultas Universitatsverlag, Wien (Austria), pp. 33–44.

Rechtschaffen, A., Kales, A. (Eds.), 1968. A Manual of Standardized Terminology, Techniques and Scoring System for Sleep Stages of Human Subject. US Government Printing Office, National Institute of Health Publication, Washington DC.

Rodriguez, E., George, N., Lachaux, J., Martinerie, J., Renault, B., Varela, F., 1999. Perception's shadow: long-distance synchronization of human brain activity. Nature 397 (6718), 430–433.

Roelfsema, P. R., Engel, A. K., König, P., Singer, W., 1997. Visuomotor integration is associated with zero time-lag synchronization among cortical areas. Nature 385, 157–161.

Rosenblum, M. G., Pikovsky, A. S., Kurths, J., 1996. Phase synchronization of chaotic oscillators. Phys Rev Lett 76 (11), 1804–1807.

Spencer, K. M., Nestor, P. G., Niznikiewicz, M. A., Salisbury, D. F., Shenton, M. E., McCarley, R. W., 2003. Abnormal neural synchrony in schizophrenia. J Neurosci 23 (19), 7407 – 7411.

Steriade, M., Dossi, R. C., Paré, D., Oakson, D., 1991. Fast oscillations (20 - 40 Hz) in thalamocortical systems and their potentiation by mesopontine cholinergic nuclei in the cat. Neurobiology 88, 4396–4400.

Steriade, M., McCormick, D. A., Sejnowski, T. J., 1993a. Thalamocortical oscillations in the sleeping and aroused brain. Science 262, 679–685.

Steriade, M., Nuñez, A., Amzica, F., 1993b. A novel slow (<1 Hz) oscillation of neocortical neurons in vivo: Depolarizing and hyperpolarizing components. J Neurosci 13 (8), 3252–3265.

Tcheslavski, G., Beex, A., 2006. Phase synchrony and coherence analyses of EEG as tools to discriminate between children with and without attention deficit disorders. Biomed Signal Process Contr 1 (2), 151 – 161.

Theiler, J., Eubank, S., Longtin, A., Galdrikian, B., Farmer, J. D., 1992. Testing for nonlinearity in time series: the method of surrogate data. Physica D 58 (1-4), 77–94.

Torrence, C., Compo, G. P., 1998. A practical guide to wavelet analysis. Bull Amer Meteorological Society 79 (1), 61–78.

Varela, F., Lachaux, J., Rodriguez, E., Martinerie, J., 2001. The brainweb: Phase synchronization and large-scale integration. Nature Rev Neurosci 2 (4), 229–239.

Vejmelka, M., Paluš, M., 2008. Inferring the directionality of coupling with conditional mutual information. Phys Rev E 77 (2), 026214.

Winterhalder, M., Schelter, B., Kurths, J., Schulze-Bonhage, A., Timmer, J., 2006. Sensitivity and specificity of coherence and phase synchronization analysis. Phys Lett A 356 (1), 26–34.

Xu, L., Chen, Z., Hu, K., Stanley, H. E., Ivanov, P. C., 2006. Spurious detection of phase synchronization in coupled nonlinear oscillators. Phys Rev E 73 (6), 065201(R).